*High Energy Phenomena in Relativistic Outflows V*
*AAA Workshop Series 8, 2016*
*L. J. Pellizza and G. E. Romero, Eds.*

# Optical spectroscopic monitoring of the variation in the circumstellar disc in PSR B1259-63/LS 2883 during the 2014 periastron passage

B. van Soelen[1], P. Väisänen[2,3], A. Odendaal[1], I. Sushch[4,5], L. Klindt[1], P.J. Meintjes[1]

[1]*Department of Physics, University of the Free State, Bloemfontein, 9301, South Africa*
[2]*South African Astronomical Observatory, PO Box 9 Observatory, 7935, South Africa*
[3]*Southern African Large Telescope, PO Box 9 Observatory, 7935, South Africa*
[4]*Centre for Space Research, North-West University, Potchefstroom, 2520, South Africa*
[5]*Astronomical Observatory of Ivan Franko National University of LâĂŹviv, vul. Kyryla i Methodia, 8, 79005, LâĂŹviv, Ukraine*

**Abstract.** The $\gamma$-ray binary system PSR B1259-63/LS 2883 passed through periastron in May of 2014 and was the focus of intensive multi-wavelength campaigns. During the previous periastron, a large flare was detected at GeV energies 30 days after the 2010 periastron passage by *Fermi*-LAT. This event was re-detected during 2014 at a similar orbital phase. In order to place better constraints on the behaviour of the circumstellar disc around periastron, we performed optical spectroscopy of the H$\alpha$ and He I ($\lambda$6678) lines with the Southern African Large Telescope (SALT) from 33 days before until 78 days after the 2014 periastron. The H$\alpha$ line remains single peaked through all observations, but with a noted asymmetry and variation in shape. The He I line remains double peaked and shows a variation in the relative peak heights. Both lines show an increase in the equivalent width which peaks after periastron. The line strengths before periastron are, however, weaker than were detected around the 2010 periastron, though are comparable after periastron.

## 1. Introduction

The $\gamma$-ray binary system PSR B1259-63/LS 2883 consists of a 48 ms pulsar in an approximately 3.4 year orbit around the Be star LS 2883 (Johnston et al. 1992). The interaction between the pulsar and stellar winds leads to the formation of a shock, resulting in non-thermal radio, X-ray and $\gamma$-ray emission, which is strongest around periastron. The presence of a circumstellar disc around LS 2883 alters the interaction region when the pulsar passes close to the disc, (inferred by the eclipse of the pulsed radio signal). Over the last two periastron passages observations with *Fermi*-LAT have detected a flare-like event starting approximately 30 days after periastron (e.g. Abdo et al. 2011, Caliandro et al 2015, Tam et al. 2015) at a phase when the other non-thermal emission is de-

creasing. However, there is an indication of a multi-wavelength component, as a hardening in the X-ray emission has been noted around the period of the *Fermi* flare (e.g. Chernyakova et al. 2015). Since the interaction between the pulsar and disc near the second disc crossing could have an important effect on the non-thermal emission, it is important to follow the variation in the circumstellar disc around periastron. For an approximately three month period around the 2014 periastron, which occurred on the 4th of May 2014 (MJD 56781.42), we observed the binary system with the Southern African Large Telescope (SALT) as well as with the SAAO 1.9-m telescope. Below we briefly discuss SALT as well as summarize the results of the optical observations reported in van Soelen et al. (2016) and Chernyakova et al. (2015).

## 2. The Southern African Large Telescope

The South African Astronomical Observatory (SAAO) operates and manages the optical and infrared telescopes located at the Sutherland station, located in the Northern Cape, South Africa (32.38°S, 20.81°E). This includes the Southern African Large Telescope (SALT) as well as a number of smaller telescopes.

SALT, a 10 metre class telescope, was built between 2000-2005, following a similar design as the Hobby-Eberly Telescope (HET). The primary mirror, which consists of 91 hexagonal segments, has a fixed elevation angle of 37° relative to the zenith, which greatly reduced the cost of construction. Due to this design observations are limited to declinations between $+10°$ to $-72°$. The tracking of astronomical sources is achieved by moving the science instruments located at the prime focus and the track time is between 1 to 3 hours, depending on the declination of the target (O'Donoghue et al. 2006, 2008).

SALT is currently equipped with four instruments: SALTICAM, the Robert Stobie Spectrograph (RSS), the High Resolution Spectrograph (HRS) and a visitor instrument, the Berkeley Visible Image Tube camera (BVIT).

*SALTICAM* This is the primary imager instrument on SALT. The detector consists of two mosaicked 2048×4012 pixel E2V Technologies CCDs (see e.g. O'Donoghue et al. 2006). The system is specifically chosen to be sensitive in the ultra-violet and optical range. The plate scale at the detector is 0.14 arcsec/pixel, with an 8 arcmin diameter science usable field of view.

*RSS* The three main modes of operation of the RSS are long-slit spectroscopy, multi-object spectroscopy and Fabry-Perot imaging spectroscopy (e.g. Kobulnicky et al. 2003). The fourth mode, spectro-polarimetry is currently being commissioned. The spectrograph is equipped with six diffraction gratings, which are operated in first order. Standard long-slit spectroscopy can be performed with a selection of 7 slits which range in width from 0.6 to 4 arcseconds. Multi-object spectroscopy is performed by using slits that are laser cut into a carbon fibre mask, allowing for the spectra of multiple objects to be extracted in a single observation. The Fabry-Perot (e.g. Rangwala et al. 2008) is available in low-resolution, medium-resolution, high-resolution and tunable filter modes.

*HRS* The High Resolution fibre-feed échelle spectrograph (e.g. Crause et al. 2014), has a wavelength coverage of 3700–5550 Å and 5550–8900 Å on two sepa-

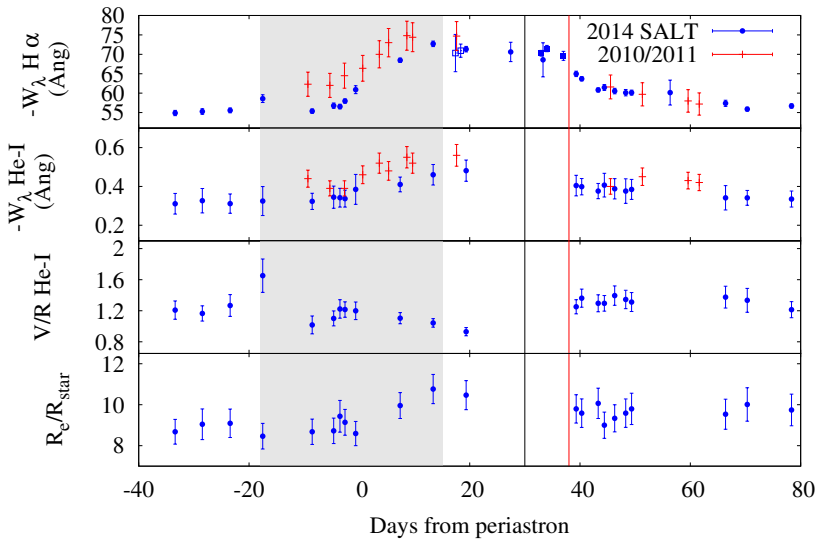


Figure 1. Equivalent width of the H$\alpha$ (top), and equivalent width, V/R variation and emission location of He I as observed with SALT in 2014 (blue circles, van Soelen et al. 2016). The 2010/2011 observations are shown for comparison (Chernyakova et al 2014). Also shown are observations undertaken with the SAAO 1.9-m (blue open squares, van Soelen et al. 2016, filled squares Chernyakova et al. 2015). The black and red vertical lines show the time of the onset and peak of the 2014 *Fermi* flare, respectively (Caliandro et al. 2015). The shade region indicates the period of the pulsar eclipse (Chernyakova et al 2014).

rate channels. The spectrograph can operate in four modes, namely, low resolution ($R \sim 15000$), medium resolution ($R \sim 40000$), high resolution ($R \sim$ 65000) and high stability ($R \sim 65000$, optimized for radial velocity measurements).

*BVIT* This visitor instrument is a very high time resolution (< 1 microsecond) photon counting camera (e.g. Siegmund et al. 2008).

## 3. Observations of the PSR B1259-63/LS 2883

The $\gamma$-ray binary system PSR B1259-63/LS 2883 was observed with SALT using the RSS from 33 days before (30 April 2014) until 78 days after (21 July 2014) the 2014 periastron passage. The RSS was configured to observe 6176.6 – 6983.0 Å to focus on the H$\alpha$ and He I lines. Each observation consisted of 3 to 4 exposures for a total integration time of $\sim$ 500 seconds, achieving a signal to noise ratio of $\sim$ 200. The H$\alpha$ emission line was also observed with the SAAO 1.9-m telescope between 17–18 days (van Soelen et al. 2016) and 33–38 days (Chernyakova et al. 2015) after the 2014 periastron.

Both the H$\alpha$ and He I lines remain in emission through all observations, with $W_{\lambda,\mathrm{H}\alpha} \approx -61$ Å and $W_{\lambda,\mathrm{He}} \approx -0.57$ Å over the observation period. The

H$\alpha$ line is an asymmetric, single peaked emission line, while the He I line shows a double peaked emission line, superimposed on the underlying stellar absorption line. The orbital variations of the lines around the 2014 periastron are shown in Fig. 1 (blue points) in comparison to the 2010 periastron (red points). There is a marked change in the asymmetry and an increase in the equivalent width at 17 days before periastron, with an increase in the violet component. This occurs around the time of the first disc crossing.

The V/R variation of the He I shows an increase in the asymmetry around the first disc crossing, a general decrease in V/R after periastron, with the red component becoming slightly stronger (V/R = $0.93 \pm 0.05$) around the second disc crossing. From the change in the separation of the V&R peaks we have calculated the location of the He I emission in the circumstellar disc (Huang 1972). This shows the emission location varies between $8.3 < R/R_\star < 10.8$ around periastron (Fig. 1), moving further out in the disc around periastion, to a maximum around the same period as the maximum equivalent width.

## 4. Discussion & Conclusion

The observations confirm the general trend previously observed for PSR B1259-63/LS 2883, with an improvement in the orbital phase coverage. The H$\alpha$ EW is lower than the 2010 observations which we suggest is due to the intrinsic variability associated with the Be star. This may indicate a lower mass for the disc around the 2014 periastron passage. A more detailed description is given in van Soelen et al. (2016). From a comparison to multi-wavelength results around this period it has been suggested that there is a change in the mass of the disc during the period following the *Fermi* flare (e.g. Chernyakova et al. 2015).

**Acknowledgments.** PV acknowledges the support of the NRF.

## References

Abdo A.A., et al. 2011 ApJ, 736, L11
Caliandro G.A., et al. 2015, ApJ, 811, 68
Chernyakova M., et al. 2014, MNRAS, 439, 432
Chernyakova M., et al. 2015, MNRAS, 454, 1358
Crause, L.A. et al. 2014, SPIE, 9147, 6
Huang S. 1972, ApJ, 171, 549
Johnston S., et al. 1992, ApJ, 387, L37
Kobulnicky H.A., et al. 2003 SPIE, 4841, 1634
O'Donoghue D. et al., 2006, MNRAS, 372, 151
O'Donoghue D. et al., 2008, SPIE, 7018, 13
Rangwala N., Williams T.B., Pietraszewski C., Joseph C.L., 2008, AJ, 135, 1825
Siegmund O.H.W.S., et al. 2008, AIP Conf. Proc., 984, 103
Tam P.H.T., et al. 2015, ApJ, 798, L26
van Soelen B. et al., 2016, MNRAS, 455, 3674